CHEMISTRY
A EUROPEAN JOURNAL

DOI: 10.1002/chem.201000595

Self-Assembled Ultralong Chiral Nanotubes and Tuning of Their Chirality Through the Mixing of Enantiomeric Components

Xuefeng Zhu,[a] Yuangang Li,[a, b] Pengfei Duan,[a] and Minghua Liu*[a]

Abstract: Enantiomeric L- or D-glutamic acid based lipids were designed and their self-assembly was investigated. It was found that at a certain concentration, either L- or D-enantiomeric derivatives could self-assemble in absolute alcohol to form a white organogel, which was composed of ultralong nanotubes with an aspect ratio higher than 1000. Further investigations revealed that these nanotubes were in chiral forms. The chirality of the nanotubes was determined by that of the enantiomers employed. In addition, when D and L enantiomers were mixed in different ratios, the nanotube could be tuned consecutively from nanotubes with a helical seam to nanotwists, the chirality of which being determined by the excess enantiomer in the mixed systems. In the case of an equimolar mixture of the enantiomers, flat nanoplates instead of helical nanotubes or nanotwists were obtained. The FTIR vibrational data and XRD layer-distance values showed a consecutive change as a function of the enantiomeric excess. It was further revealed that the slightly stronger interaction between D–L enantiomeric pairs than that between D–D or L–L pairs was responsible for the formation of the diverse self-assembled nanostructures.

Keywords: chirality · lipids · nanostructures · self-assembly · supramolecular chemistry

Introduction

Lipid nanotubes have been attracting great interest due to their unique structural features,[1] their use as templates for synthesizing one-dimensional nanomaterials,[2] and their potential as drug delivery nanocarriers.[3] The first lipid nanotube was suggested to be self-assembled from 1,2-bis(10,12-tricosadiynoyl)-*sn*-glycero-3-phosphocholine.[4] Since then, various organic amphiphiles such as phospholipids,[5] glutamate,[6] glycolipids,[7] peptide lipids,[8] and others[9] have been designed to construct lipid nanotubes. During the formation of these nanotubes, the chirality is a frequently encountered important issue.[1,2,10] Both theoretical models[11] and experimental results[8c,12] indicate that the molecules experience chiral packing to form the high-curvature nanotubes. In addition, the chiral nanotubes can mimic some biological systems.[1,2,13] Therefore, controlling the chirality of the nanotubes is very important. An efficient way to control the chirality of the nanotube is to introduce chiral molecules to the self-assembling system.[1,2,10] Besides chiral amphiphiles, the combination of achiral amphiphiles and chiral counterions also proved to be an effective alternative.[14] Furthermore, through the mixing of certain enantiomers with opposite chirality, nanotubes with tunable chirality can be expected. Oda et al. reported an excellent example of tunable chirality in the mixing system of gemini amphiphiles containing counterions with opposite chirality.[14] Although the mixing of two enantiomers is expected to give a more direct control over the chirality as well as the morphology of the resulting nanotubes, most studies focus on a 1:1 mixture of enantiomers or racemates,[14c] which tends to form either a mixture of right-handed and left-handed helices[15] or platelets[16] and tubular[17] structures that do not express macroscopic chirality. Unfortunately, detailed data concerning the assembling behavior of enantiomers other than 1:1 mixtures are scarce. Herein, we describe how we designed two enantiomeric lipids with opposite chirality and directly tuned the chirality as well as the morphology of the lipid nanotubes through

[a] X. Zhu, Dr. Y. Li, P. Duan, Prof. Dr. M. Liu
Beijing National Laboratory for Molecular Science
CAS Key Laboratory of Colloid
Interface and Chemical Thermodynamics
Institute of Chemistry, Chinese Academy of Sciences
Beijing, 100190 (P.R. China)
E-mail: liumh@iccas.ac.cn

[b] Dr. Y. Li
Present address:
College of Chemistry and Chemical Engineering
Xi'an University of Science and Technology
Xi'an, 710054 (P.R. China)

Supporting information for this article is available on the WWW under http://dx.doi.org/10.1002/chem.201000595.

mixing of the two simple enantiomers at various molar ratios. These consecutive changes of the chirality in the mixed systems were further confirmed by the characteristic vibration bands and distances between the layers of molecular-level chiral interactions. Such tuning of the chirality as well as the morphology may provide an important clue for the folding and unfolding of proteins.

Results and Discussion

Molecular design: The molecular structure of the designed amino acid based lipids, *N*,*N*′-bis(octadecyl)-L-glutamic diamide (LGAm) and its enantiomer DGAm, is shown in Figure 1a. The enantiomers were synthesized from the amidation of the *tert*-butoxycarbonyl (Boc)-protected L- or D-glutamic acid with octadecylamine, followed by elimination of the Boc group to free the amino group.[18] With such a molecular design, the compounds possess a head group with multiple hydrogen-bond sites, such as the amide and free amino groups, and two saturated alkyl tails with strong hydrophobic interactions. These potential hydrogen-bond sites make it easy for the enantiomers to self-assemble. In addition, the hydrogen-bonding interactions between the homochiral enantiomers might be slightly different from those between heterochiral enantiomers, which could lead to different morphologies.

Self-assembly of pure enantiomer: The self-assembly of the compounds proceeds through a solvent-mediated process. At room temperature, only a small amount of the compound dissolved in ethanol. Upon heating to the boiling point of ethanol, the compounds became soluble and formed a transparent solution. After cooling down to room temperature, precipitates or organogels were formed depending on the concentration of the solution.

When the concentration was less than 1 mg mL^{-1} (0.0015 M), a precipitate was essentially formed. White opaque organogels were always formed when the concentration exceeded 19.5 mg mL^{-1} (0.03 M); this was confirmed by inverting the test tube and no solvent flowed (Figure S1 in the Supporting Information). This means that the critical gelation concentration (CGC) of the amphiphile is 0.03 M or so. Since the precipitate could separate out from quite a dilute solution (1 mg mL^{-1}, 0.0015 M), organized structures are suggested to be formed even before the CGC. Therefore, we have recorded the scanning electron microscopy (SEM) and transmission electron microscopy (TEM) images for the LGAm samples prepared from either the xerogel or the air-dried suspensions formed at lower concentrations.

Figure 1 shows the morphological pictures of the nanostructures formed under different conditions. At a low concentration of 1 mg mL^{-1}, various nanostructures are formed. Nanosheets are essentially formed with some twisted nanostrips and nanotubes. The nanotubes are not uniform and some bamboo-like morphologies are observed. Upon increasing the concentration of the solution, similar nanostructures with an increased number of nanotubes were formed. Perfect nanotubes with higher aspect ratio and uniform diameter as well as thickness were obtained when the concentration of LGAm was increased to 20 mg mL^{-1}. The TEM images indicate that the nanotubes have a wall thickness of

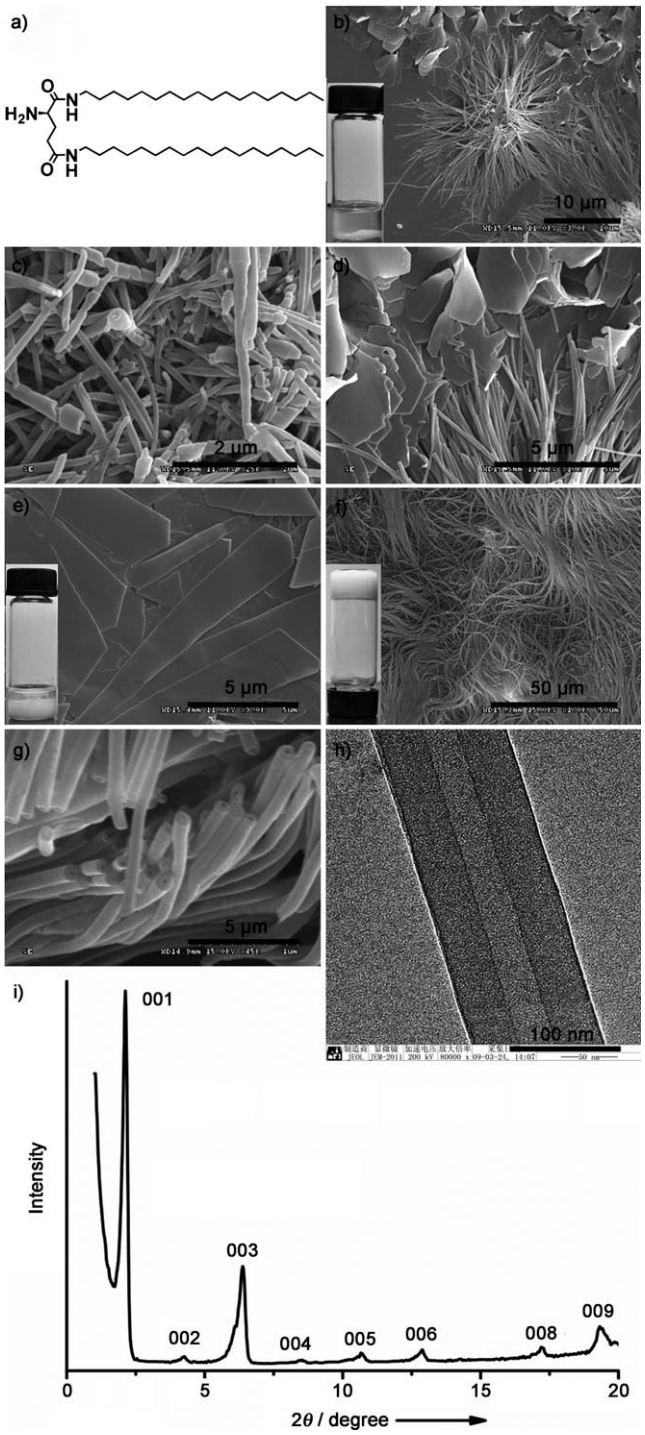

Figure 1. a) Molecular structure of the enantiomer of LGAm. b)–g) SEM images of self-assembled LGAm nanostructures from ethanol under different conditions: b),c),d) 0.0015 M, e) 0.03 M before gelation, f),g) 0.03 M after gelation. h) TEM images for the organogels formed by LGAm with ethanol at 0.03 M. i) XRD of LGAm xerogel from ethanol.

(45.6±1.0) nm, an outer-sphere diameter of (116.7±1.3) nm, and an inner sphere of (23.7±1.2) nm. The length of the nanotubes extends to several-hundred micrometers, with an aspect ratio greater than 1000 (see Figure S2 in the Supporting Information).

To further disclose the structures of the nanotubes, the xerogel was cast on quartz plates and measured using X-ray diffraction (XRD). Well-defined diffraction patterns were observed and all these diffraction peaks can be assigned as 00*l* diffractions, which extend to 0012 (Figure 1i showed only to 009). According to the Bragg equation $2d\sin\theta = n\lambda$, the layer distance is estimated to be 4.16 nm. Based on the CPK space-filling model of the compound, this value corresponds to the *d*-spacing value of LGAm in a bilayer structure. Since the width of the nanotubes is around 45 nm, as revealed by TEM images, it can be inferred that the nanotubes were rolled up from the orderly accumulated multiple bilayers (10 bilyers or so). For LGAm, the rolling direction is always in the right-handed sense as shown in Figure 1c.

The D enantiomer (DGAm) showed the same self-assembly behavior (see Figure S3 in the Supporting Information) and the formed nanotubes have a wall thickness of (36.6±5.4) nm, an outer diameter of (101.6±3.4) nm, and an inner diameter of (24.4±3.0) nm. As expected, these nanotubes showed an opposite chirality, which is a left-handed one. To sum up, the L enantiomer formed right-handed nanotubes whereas the D enantiomer made left-handed ones. This further indicates that the pure enantiomeric lipid molecules adopted a chiral-packed form in these self-assembled nanotubes, the supramolecular chirality of which was determined by the chirality of the corresponding molecule.[1b,12d]

Tuning chirality and morphologies: Interestingly, when we mixed the two enantiomers in different proportions, the morphologies of the self-assembled nanostructures showed a continuous change from left-handed nanotubes through twist ribbons and nanosheets to right-handed nanotubes along with an increase of the enantiomeric excess values in succession. The chirality of the nanotubes can be tuned by the choice of enantiomer and such change is clearly shown in Figure 2. Previously, Oda[14] et al. realized tunable chirality by mixing chiral tartrate with cationic gemini amphiphiles. It was suggested that the continuous mixing of enantiomers is unique to tartrate amphiphiles because simply mixing enantiomers of chiral amphiphiles generally leads to the precipitation of the racemate or to their phase separation in helices of opposite handedness.[14c] Fortunately, with rational design of the molecules, we, for the first time, have shown that the mixing of two simple enantiomers is also effective in tuning the chirality of the formed nanotubes.

Figure 2 shows the SEM pictures of such mixtures with various ratios of the enantiomers. Several important features are seen. First, whereas the pure enantiomers formed perfect nanotubes, the mixture showed a difference in their nanostructures. When 5% L enantiomer was mixed with 95% D enantiomer, the nanotubes still formed with a clear left-handed helical seam. The nanotubes changed into nano-

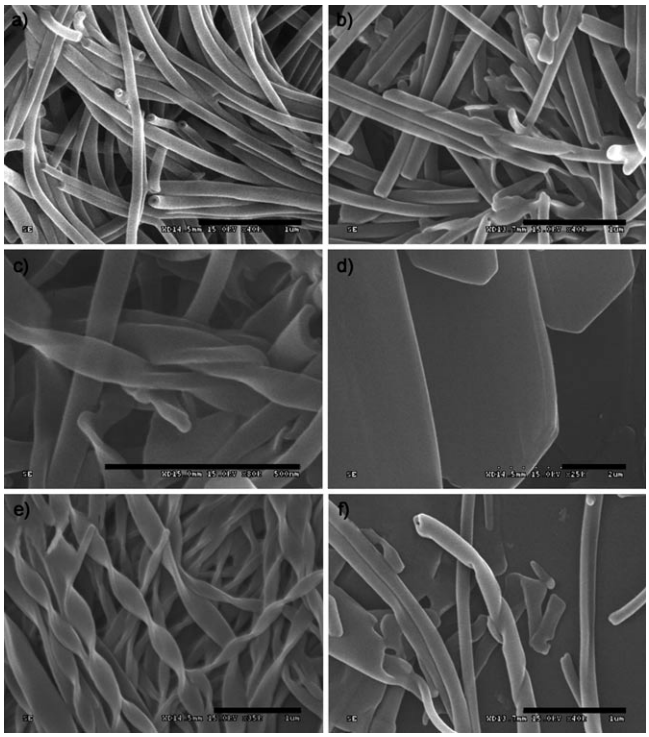

Figure 2. SEM images of DGAm/LGAm gels at different molar ratios (D/L): a) 100:0 (pure DGAm), b) 95:5, c) 75:25, d) 50:50, e) 25:75, f) 5:95. Scale bars: 1 μm.

twists, but still with left-handedness, when 25% of the L-enantiomer was used. With a further increase of the proportion of L enantiomer, the twist became weak. In a 1:1 mixture, a uniform plate was observed instead of the twist. When the L enantiomer was used in an excess amount in mixtures, the twist was observed again but with changed handedness. When the amount of the L enantiomer reached 95%, right-handed helical nanotubes were formed. These morphological changes clearly demonstrated a serial tuning of the chirality of the resulting twists and nanotubes. The results further revealed that the chiral nanostructures were clearly determined by the chirality of the major component, that is, the chirality of the nanostructure obeys the "majority rule".[19]

FTIR studies: To get further insight into the mixing effect, FTIR spectra were obtained for the nanostructures formed at different mixing ratios, as shown in Figure 3 and Table 1. For the pure enantiomer, for either LGAm or DGAm, the asymmetric and symmetric CH_2 stretching vibrations appeared at 2919 and 2851 cm^{-1}, respectively, which suggests that the alkyl chain packed in an all-*trans* conformation.[20] The stretching vibration of the N–H was observed at around 3326 cm^{-1}, which indicates that both the amino groups and the amide groups are in the hydrogen-bonded form.[8c,12c] All the amide I and amide II bands appeared at around 1636 and 1532 cm^{-1}, which indicates that both C=O and N–H are in the hydrogen-bonded form, too.[8c,12c] These FTIR spectral

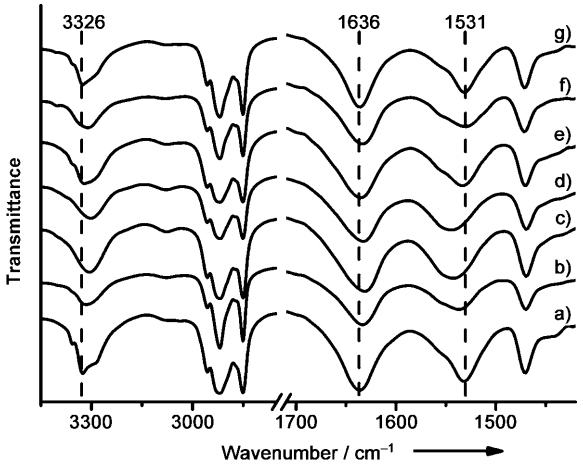

Figure 3. FTIR spectra of DGAm/LGAm gels at different molar ratios (D/L): a) 100:0, b) 95:5, c) 75:25, d) 50:50, e) 25:75, f) 5:95, g) 0:100.

Table 1. Main vibration bands [cm^{-1}] in the FTIR spectra of DGAm/LGAm gels at different molar ratios.

D/L[a]	νNH	$\nu(CH_2)n$	Amide I	Amide II	$\delta(CH_2)$
0:100	3326	2919, 2851	1636	1531	1471
5:95	3311	2919, 2851	1633	1530	1471
25:75	3306	2919, 2851	1631	1543	1469
50:50	3302	2918, 2851	1633	1544	1469
75:25	3306	2919, 2850	1631	1543	1470
95:5	3315	2919, 2851	1633	1537	1470
100:0	3326	2919, 2851	1636	1532	1471

[a] D/L denotes DGAm/LGAm at different molar ratios; 0:100 is pure LGAm and 100:0 is pure DGAm.

features indicate that multiple hydrogen bonds between head groups together with the closely packed tails among the pure enantiomeric molecules are the driving force for the formation of chiral multi-bilayers and supramolecular nanotubes.

When different molar ratios of the L and D enantiomers were mixed, the FTIR spectra showed an interesting variation: the asymmetric and symmetric stretching vibrations of CH_2 always appeared at 2919 and 2851 cm^{-1}, respectively, which suggested that the alkyl chains are still closely packed in an all-*trans* conformation.[20] This indicates that in the enantiomeric mixtures, the alkyl tails of DGAm molecules could contact those of the LGAm molecules in the same way as in pure enantiomers (DGAm or LGAm). However, the N–H stretching vibrations tended to shift to lower wavenumbers, and the amide I and amide II simultaneously shifted to lower and higher wavenumbers, respectively. In the case of a 50:50 mixture, we see the largest wavenumber shifts, that is, the N–H vibration has shifted to 3302 cm^{-1}, and the amide I and amide II to 1633 and 1544 cm^{-1}, respectively. In pure enantiomer assemblies, the hydrogen bond is based on the head groups of L–L or D–D pairs; whereas in mixtures of D and L enantiomers, the hydrogen bond could also occur between the D–L pairs. The changes of the vibration bands in the enantiomeric mixture indicate that upon mixing, the hydrogen-bonding interactions between D and L enantiomers (D–L pairs) are stronger than those between L–L pairs or D–D pairs.

XRD studies: As discussed above, perfect nanotubes are composed of multiple bilayers as revealed by X-ray diffraction. X-ray diffraction analyses were also carried out for the other assemblies (Figure 4). It was found that orderly, organized bilayer structures essentially existed in every enantiomeric mixture regardless of the composition. Although some of the xerogels showed two kinds of *d*-spacing values, which might be due to the deviated packing of the alkyl chain, *d*-spacing values showed a similar consecutive change relative to the mixing ratios. That is, there was a minimum layer distance for pure enantiomer (4.16 nm for LGAm), and a maximum value for the racemic mixture (4.85 nm for DGAm/LGAm = 50:50 (mol%)). This means that during the self-assembly through hydrogen bonds, the chiral interactions between the enantiomeric molecules cause them to pack at a nonzero angle with respect to their nearest neighbors.[1b] In the intermediate multi-bilayers, a large number of such chiral interactions accumulate more and more, so that when the helical torsion force becomes strong enough, it causes the layer structures to twist in one energetically preferable orientation.[12d] The intermediate multi-bilayers ultimately roll into chiral nanotubes (here, LGAm made right-handed ones and DGAm formed left-handed ones). It is clear that for pure enantiomers, the molecules were in the torsional conformation most suited to their chiral nature and the helical torsion force was the strongest in their bilayers. And thus, perfect chiral nanotubes without any helical seams were finally formed and the minimum *d*-spacing value of the bilayers was obtained. When a certain amount of the opposite handed enantiomer was involved, the formation of racemic D–L pairs formed took priority since the hydrogen bonds of D–L pairs are stronger than those of either L–L or D–D pairs. This means that the helical torsion force

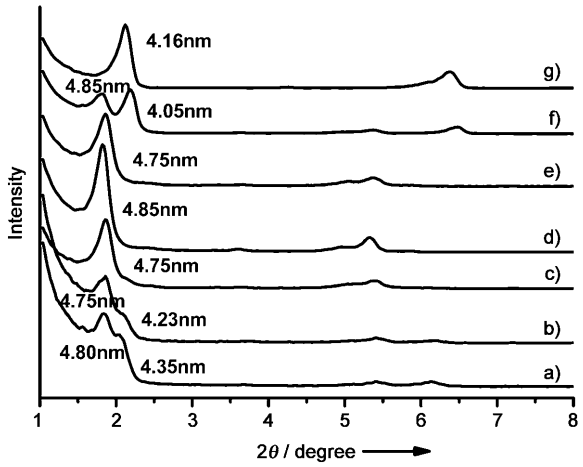

Figure 4. X-ray diffraction spectra of DGAm/LGAm gels at different molar ratios (D/L): a) 100:0, b) 95:5, c) 75:25, d) 50:50, e) 25:75, f) 5:95, g) 0:100.

among the resulting layer structures decreased. Therefore, the helical seams of the nanotubes survived in the 95:5 or 5:95 mixtures and nanotwists formed when more enantiomers with opposite chirality were involved. In the racemic mixtures, the chiral interaction between racemic D–L pairs was stronger and the interactions between D–D or L–L pairs were suppressed. In this case, no helical torsion force existed throughout the entire bilayers. Thus, only flat plates as well as the maximum *d*-spacing value of the bilayers was obtained.

Assembly mechanism: To better understand the role of the chiral interaction in such hierachical self-assemblies, we can view all these data with respect to the enantiomeric excess. The enantiomeric excess has been used to evaluate the chirality effect,[14a] which is defined here as $E_{D/L}=(\Phi_L-\Phi_D)/(\Phi_L+\Phi_D)$, in which Φ_L and Φ_D are the relative molar concentrations of LGAm and DGAm, respectively. The $E_{D/L}$ value can be from −1 to 1, which represents the pure D or L enantiomer, respectively. An $E_{D/L}$ value of zero means a racemic mixture of LGAm and DGAm.

Figure 5 shows a correlation of several experimental data of the self-assembled nanostructures, such as the vibration bands of the N−H stretch, amide I and amide II, and the layer distances to the $E_{D/L}$ values. Clearly, every one of these parameters showed a nearly symmetrical curve in a U shape or inverse-U shape (∩ shape), with a minimum or maximum value at $E_{D/L}=0$. This clearly indicated that in the enantiomeric mixtures, the D–L interaction is stronger than that of either the L–L or D–D interaction. Therefore, the strongest hydrogen bond and the lowest *d*-spacing value of bilayers emerged in the racemic mixtures. Subsequently, achiral flat nanoplates were formed. Once a small excess of one enantiomer exists, the balance of the chiral interaction between two enantiomers will be broken in the resulting bilayers. As a result, the chiral nature of the molecular blocks (LGAm or DGAm) is expressed in the supramolecular-level structures, and nanotwists or helical nanotubes were formed. In the case of the pure enantiomers, seamless nanotubes were obtained.

Based on these results and analyses, the formation and tuning of the chirality of the nanotubes can be illustrated as shown in Scheme 1. The lipid molecules have strong hydrogen bonds between the head groups as well as hydrophobic interactions among the tails and are packed into intermediate plates, which consist of many bilayers. Due to the chiral nature of the formed layers, the plate rolls up into a nanotube. Since the nanoplates were composed of multiple bilayer structures as repeat units, they rolled into very long and multilayered thick-walled nanotubes. The handedness of the molecules controlled the chirality of the nanotube. Thus, an L enantiomer formed a right-handed nanotube, whereas a D enantiomer formed a left one. When two enantiomers were mixed, the interactions between the L–L or D–D enantiomers were weaker than those between the D–L enantiomers. Thus, D–L preferred to mix with each other. Such mixing caused the formation of the multibilayer plate structures, as verified by the 1:1 mixtures. Since there is no enantiomeric excess, the 1:1 mixture formed the plate only. However, when there is an excess of an enantiomer, the plate twists, and the direction of the twist is determined by the excess enantiomer, which means the coassembly of the enantiomers obey the "majority rule". Thus, upon mixing the enantiomers in different ratios, we are able to tune the chirality of the nanotubes and realize hierachical self-assemblies.

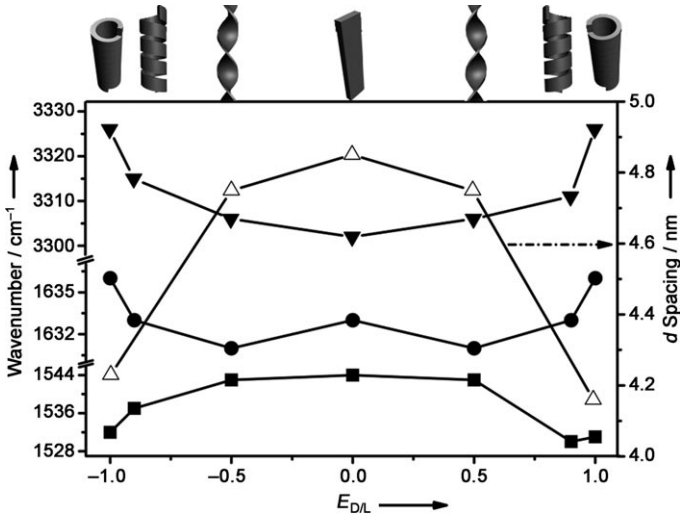

Figure 5. The correlative plot of the vibration bands of N−H, amide I, and amide II and the *d* spacing of the nanostructures in the mixed gels against the enantiomeric excess value ($E_{D/L}$): (▼) the stretching vibration bands of N−H; (●) the amide I bands; (■) the amide II bands; (△) the *d*-spacing values. The cartoon upside is the relevant morphologies of the self-assembled nanostructures.

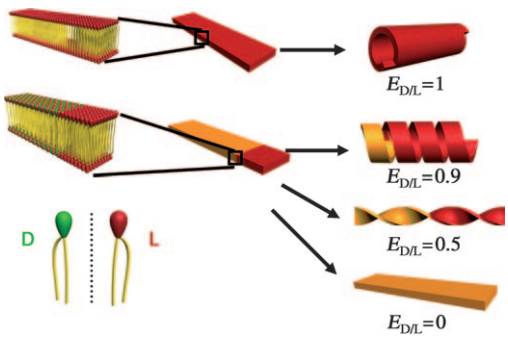

Scheme 1. The proposed mechanism for the formation of various nanostructures. The red and green head groups represent the L and D enantiomers, respectively. When pure L enantiomer self-assembled, a helical nanotube was formed (top). When some D enantiomer (green) was added, some of the enantiomers formed the racemate (yellow). The excess amount of L enantiomer drove the formation of nanotubes with a helical seam (right, second from the top) and twists. When equimolar amounts of enantiomers were mixed ($E_{D/L}=0$), only a plate was formed (bottom). Here only one bilayer out of the multi-bilayers is showed for clarity.

Conclusion

Two enantiomeric L- or D-glutamic acid based lipids were designed. The pure enantiomers could self-assemble into ultralong helical nanotubes in ethanol through gel formation, and the chirality of the gel is determined by the chirality of the enantiomer. When the two enantiomers were mixed in different ratios, the self-assembled nanostructures experienced morphological changes from nanotubes to nanotubes with a helical seam, nanotwists, and finally nanosheets and the chirality of these nanostructures was able to be tuned by the excess enantiomer. A series of characterizations such as SEM, TEM, FTIR, and XRD revealed that the chiral interactions in these enantiomers played an important role in forming the corresponding nanostructures. The slightly stronger interactions between D–L enantiomeric pairs relative to that of D–D or L–L pairs determined the formation of the diverse self-assembled nanostructures.

Experimental Section

Instruments and methods: ^{1}H NMR spectra were recorded on a Bruker AV400 spectrometer. Matrix-assisted laser desorption ionization time-of-fight mass spectrometry (MALDI-TOF MS) were recorded on a BIFLEIII instrument. Elemental analysis was performed on a Carlo–Erba-1106 instrument. Scanning electron microscopy (SEM) was performed on a Hitachi S-4300 FE-SEM microscope and transmission electron microscopy (TEM) images were obtained on a JEM-2011 electron microscope operating at accelerating voltages of 15 and 200 kV, respectively. Fourier transform infrared (FTIR) spectra were recorded on a Bruker Tensor 27 FTIR spectrometer at room temperature. X-ray diffraction (XRD) was achieved on a Rigaku D/Max-2500 X-ray diffractometer (Japan) with $Cu/_{K\alpha}$ radiation ($\lambda = 1.5406$ Å), which was operated at 45 kV, 100 mA.

Chemicals and synthesis: All commercial chemicals were used as received. The synthesis and characterization of the precursors *N,N′*-bisoctadecyl-L-Boc-glutamicdiamide (LBG) and *N,N′*-bisoctadecyl-D-Boc-glutamicdiamide (DBG) have been reported previously by our group.[18a]

***N,N′*-Bisoctadecyl-L-aminoglutamicdiamide (LGAm)**:[18b] LBG (3.575 g, 4.77 mmol) in CH_2Cl_2 (50 mL) and trifluoroacetic acid (TFA; 8 mL) was stirred at room temperature for 3 h. Then, after removal of CH_2Cl_2 and excess TFA using a rotary evaporator, the remains were dissolved in tetrahydrofuran (THF), and subsequently poured into the prepared saturated $NaHCO_3$ aqueous solution to get a white solid suspension. This was filtered and vacuum dried to give the crude product (2.990 g). Recrystallization in THF (3×80 mL) afforded the white pure product (2.600 g, 83.95%). ^{1}H NMR ($CDCl_3$, 400 Hz): $\delta = 0.86$–0.89 (t, 6H), 1.25 (m, 60H; CH_2), 1.47–1.50 (m, 4H; CH_2), 1.85 (s, 2H; NH_2), 1.92–1.97 (q, 2H; CH_2), 2.30–2.35 (m, 2H; CH_2), 3.19–3.25 (m, 4H; CH_2), 3.43–3.47 (t, 1H; CH), 6.11 (s, 1H; NH), 7.36 ppm (s, 1H; NH); MALDI-TOF MS: *m/z* calcd for $C_{41}H_{83}N_3O_2$: 650.12 $[C_{41}H_{83}N_3O_2+Na]^+$, 672.64 $[C_{41}H_{83}N_3O_2+K]^+$, 688.75; found: 650.8 $[C_{41}H_{83}N_3O_2+Na]^+$, 672.8 $[C_{41}H_{83}N_3O_2+K]^+$, 688.8; elemental analysis calcd (%) for $C_{41}H_{83}N_3O_2$: C 75.75, H 12.87, N 6.46; found: C 75.59, H 12.67, N 6.20.

***N,N′*-Bisoctadecyl-D-aminoglutamicdiamide (DGAm)**:[18b] DBG (3.482 g, 4.64 mmol) in CH_2Cl_2 (50 mL) and TFA (8 mL) was stirred at room temperature for 3 h. Then, after removal of CH_2Cl_2 and excess TFA using a rotary evaporator, the remains were dissolved in THF, and subsequently poured into the prepared saturated $NaHCO_3$ aqueous solution to get a white solid suspension. This was filtered and vacuum dried to give the crude product (2.900 g). Recrystallization in THF (3×80 mL) afforded the white pure product (2.535 g, 84.02%). ^{1}H NMR ($CDCl_3$, 400 Hz): $\delta = 0.86$–0.89 (t, 6H), 1.25–1.28 (m, 60H; CH_2), 1.47–1.50 (m, 4H; CH_2), 1.75 (s, 2H; NH_2), 1.91–1.97 (q, 2H; CH_2), 2.30–2.34 (m, 2H; CH_2), 3.19–3.25 (m, 4H; CH_2), 3.42–3.45 (t, 1H; CH), 6.12 (s, 1H; NH), 7.36 ppm (s, 1H; NH); MALDI-TOF MS: *m/z* calcd for $C_{41}H_{83}N_3O_2$: 650.12 $[C_{41}H_{83}N_3O_2+Na]^+$, 672.64 $[C_{41}H_{83}N_3O_2+K]^+$, 688.75; found: 650.8 $[C_{41}H_{83}N_3O_2+Na]^+$, 672.8 $[C_{41}H_{83}N_3O_2+K]^+$, 688.8; elemental analysis calcd (%) for $C_{41}H_{83}N_3O_2$: C 75.75, H 12.87, N 6.46; found: C 75.54, H 12.55, N 6.41.

Self-assembly experiments: A certain amount of pure LGAm with 1 mL absolute alcohol (the molar concentration of LGAm was 0.0015, 0.005, 0.01, 0.02, 0.0275, 0.03, 0.04, 0.07 mol L^{-1}) was put into a seal-capped vial and heated up to 75°C for 3 min to make a uniform transparent solution. After the solution had been spontaneously cooled down to room temperature (25°C, the cooling rate was about 10°C min^{-1}), white precipitates were obtained from the samples with a lower concentration (0.0015, 0.005, 0.01, 0.02 mol L^{-1}) and stable opaque gels were always obtained when the concentration was higher than 0.03 mol L^{-1}, as estimated by an inversion test (the solution did not flow when the test tube was inverted). Subsequently, all the samples were left standing to let them fully age for about 12 h under ambient conditions before being measured. The same experimental procedure was carried out for DGAm. To get xerogels, the fully aging gel was transferred from sample vials to quartz plates, air dried for 30 min, and vacuum dried for 12 h.

Chirality tuning experiments: With the total molar concentration kept at 0.03 mol L^{-1}, a series of enantiomeric mixtures DGAm/LGAm at specific molar ratios (100:0, 95:5, 75:25, 50:50, 25:75, 5:95, 0:100) was put into 7 seal-capped vials and absolute alcohol (1 mL) was added, respectively. After being heated up to 75°C for 3 min to make a uniform transparent solution, and then spontaneously cooled down to room temperature (25°C, the cooling rate was about 10°C min^{-1}), 7 opaque gels with different enantiomeric compositions (−1, −0.9, −0.5, 0, 0.5, 0.9, 1) were prepared and subsequently aged for about 12 h under ambient conditions before being measured.

SEM and TEM measurements: The fully aging gel was cast onto single-crystal silica plates (Pt coated) and carbon-coated Cu grids (unstained), and the trapped solvent in the gel was evaporated under ambient conditions first, and then vacuum dried for 12 h. After that, the measurements were obtained on Hitachi S-4300 FE-SEM and JEOL EM-2011 instruments operating at accelerating voltages of 15 and 200 kV, respectively.

XRD and FTIR spectra: Xerogel films on quartz plates were used for the XRD measurements, which were performed on a Rigaku D/Max-2500 X-ray diffractometer (Japan) with $Cu_{K\alpha}$ radiation ($\lambda = 1.5406$ Å), operated at 45 kV, 100 mA. The KBr pellets made from the vacuum-dried xerogels were used for FTIR spectra measurements, which were recorded on a Bruker Tensor 27 FTIR spectrometer under ambient conditions.

Acknowledgements

This work was supported by National Basic Research Program (nos. 2007CB808005, 2006CB932101) and the National Natural Science Foundation of China (nos. 20533050, 20773141), and the Fund of the Chinese Academy of Sciences.

[1] a) J. H. Fuhrhop, W. Helfrich, *Chem. Rev.* **1993**, *93*, 1565; b) T. Shimizu, M. Masuda, H. Minamikawa, *Chem. Rev.* **2005**, *105*, 1401; c) J. M. Schnur, *Science* **1993**, *262*, 1669.

[2] a) A. M. Seddon, H. M. Patel, S. L. Burkett, S. Mann, *Angew. Chem.* **2002**, *114*, 3114; *Angew. Chem. Int. Ed.* **2002**, *41*, 2988; b) M. Llusar, C. Sanchez, *Chem. Mater.* **2008**, *20*, 782; c) Y. Zhou, T. Shimizu, *Chem. Mater.* **2008**, *20*, 625; d) Y. Zhou, *Crit. Rev. Solid State Mater.*

Sci. **2008**, *33*, 183; e) P. Ringler, W. Muller, H. Ringsdorf, A. Brisson, *Chem. Eur. J.* **1997**, *3*, 620; f) E. M. Wilson-Kubalek, R. E. Brown, H. Celia, R. A. Milligan, *Proc. Natl. Acad. Sci. USA* **1998**, *95*, 8040.

[3] a) N. J. Meilander, X. J. Yu, N. P. Ziats, R. V. Bellamkonda, *J. Controlled Release* **2001**, *71*, 141; b) L. Zarif, *J. Controlled Release* **2002**, *81*, 7; c) H. Frusawa, A. Fukagawa, Y. Ikeda, J. A. Araki, K. Ito, G. John, T. Shimizu, *Angew. Chem.* **2003**, *115*, 76; *Angew. Chem. Int. Ed.* **2003**, *42*, 72.

[4] a) P. Yager, P. E. Schoen, *Mol. Cryst. Liq. Cryst. Sci.* **1984**, *106*, 371; b) J. H. Georger, A. Singh, R. R. Price, J. M. Schnur, P. Yager, P. E. Schoen, *J. Am. Chem. Soc.* **1987**, *109*, 6169.

[5] a) B. N. Thomas, R. C. Corcoran, C. L. Cotant, C. M. Lindemann, J. E. Kirsch, P. J. Persichini, *J. Am. Chem. Soc.* **1998**, *120*, 12178; b) B. K. Mishra, C. C. Garrett, B. N. Thomas, *J. Am. Chem. Soc.* **2005**, *127*, 4254; c) S. Svenson, P. B. Messersmith, *Langmuir* **1999**, *15*, 4464; d) Y. M. Lvov, R. R. Price, J. V. Selinger, A. Singh, M. S. Spector, J. M. Schnur, *Langmuir* **2000**, *16*, 5932.

[6] a) N. Nakashima, S. Asakuma, J. M. Kim, T. Kunitake, *Chem. Lett.* **1984**, 1709; b) K. Yamada, H. Ihara, T. Ide, T. Fukumoto, C. Hirayama, *Chem. Lett.* **1984**, 1713; c) L. S. Li, H. Z. Jiang, B. W. Messmore, S. R. Bull, S. I. Stupp, *Angew. Chem.* **2007**, *119*, 5977; *Angew. Chem. Int. Ed.* **2007**, *46*, 5873.

[7] a) J. H. Fuhrhop, P. Schnieder, J. Rosenberg, E. Boekema, *J. Am. Chem. Soc.* **1987**, *109*, 3387; b) S. Kamiya, H. Minamikawa, J. H. Jung, B. Yang, M. Masuda, T. Shimizu, *Langmuir* **2005**, *21*, 743; c) G. John, J. H. Jung, H. Minamikawa, K. Yoshida, T. Shimizu, *Chem. Eur. J.* **2002**, *8*, 5494; d) J. H. Jung, Y. Do, Y. A. Lee, T. Shimizu, *Chem. Eur. J.* **2005**, *11*, 5538.

[8] a) R. C. Elgersma, T. Meijneke, G. Posthuma, D. T. S. Rijkers, R. M. J. Liskamp, *Chem. Eur. J.* **2006**, *12*, 3714; b) S. Vauthey, S. Santoso, H. Gong, N. Watson, S. Zhang, *Proc. Natl. Acad. Sci. USA* **2002**, *99*, 5355; c) M. Kogiso, S. Ohnishi, K. Yase, M. Masuda, T. Shimizu, *Langmuir* **1998**, *14*, 4978.

[9] a) K. Köhler, G. Forster, A. Hauser, B. Dobner, U. F. Heiser, F. Ziethe, W. Richter, F. Steiniger, M. Drechsler, H. Stettin, A. Blume, *J. Am. Chem. Soc.* **2004**, *126*, 16804; b) C. L. Zhan, P. Gao, M. H. Liu, *Chem. Commun.* **2005**, 462; c) R. Oda, I. Huc, S. J. Candau, *Chem. Commun.* **1997**, 2105; d) V. H. Soto Tellini, A. Jover, F. Meijide, J. V. Tato, L. Galantini, N. V. Pavel, *Adv. Mater.* **2007**, *19*, 1752.

[10] a) A. Brizard, R. Oda, I. Huc, *Top Curr Chem.* Springer, Heidelberg, **2005**, p. 167; b) M. J. Hicks, *Chirality: Physical Chemistry*; American Chemical Society Symposium Series 810; ACS, Washington, **2002**; c) A. Ajayaghosh, V. K. Praveen, *Acc. Chem. Res.* **2007**, *40*, 644; d) V. K. Praveen, S. S. Babu, C. Vijayakumar, R. Varghese, A. Ajayaghosh, *Bull. Chem. Soc. Jpn.* **2008**, *81*, 1196; e) A. Ajayaghosh, V. K. Praveen, C. Vijayakumar, *Chem. Soc. Rev.* **2008**, *37*, 109; f) A. Lohr, F. Würthner, *Chem. Commun.* **2008**, 2227; g) T. E. Kaiser, V. Stepanenko, F. Würthner, *J. Am. Chem. Soc.* **2009**, *131*, 6719; h) A. Czajlik, T. Beke, A. Bottoni, A. Perczelt, *J. Phys. Chem. B* **2008**, *112*, 7956; i) A. R. Hirst, D. K. Smith, M. C. Feiters, H. P. M. Geurts, *Chem. Eur. J.* **2004**, *10*, 5901; j) A. R. Hirst, D. K. Smith, M. C. Feiters, H. P. M. Geurts, *Langmuir* **2004**, *20*, 7070; k) B. Isare, M. Linares, L. Zargarian, S. Fermandjian, M. Miura, S. Motohashi, N. Vanthuyne, R. Lazzaroni, L. Bouteiller, *Chem. Eur. J.* **2010**, *16*, 173; l) J. Hirschberg, L. Brunsveld, A. Ramzi, J. Vekemans, R. P. Sijbesma, E. W. Meijer, *Nature* **2000**, *407*, 167; m) E. Yashima, K. Maeda, H. Iida, Y. Furusho, K. Nagai, *Chem. Rev.* **2009**, *109*, 6102; n) A. R. A. Palmans, E. W. Meijer, *Angew. Chem.* **2007**, *119*, 9106; *Angew. Chem. Int. Ed.* **2007**, *46*, 8948; o) D. Pijper, B. L. Feringa, *Soft Matter* **2008**, *4*, 1349.

[11] a) W. Helfrich, J. Prost, *Phys. Rev. A* **1988**, *38*, 3065; b) Z. C. Ouyang, J. X. Liu, *Phys. Rev. Lett.* **1990**, *65*, 1679; c) J. V. Selinger, F. C. MacKintosh, J. M. Schnur, *Phys. Rev. E* **1996**, *53*, 3804; d) B. N. Thomas, C. M. Lindemann, N. A. Clark, *Phys. Rev. E* **1999**, *59*, 3040.

[12] a) M. Caffrey, J. Hogan, A. S. Rudolph, *Biochemistry* **1991**, *30*, 2134; b) R. Oda, F. Artzner, M. Laguerre, I. Huc, *J. Am. Chem. Soc.* **2008**, *130*, 14705; c) M. Masuda, T. Shimizu, *Langmuir* **2004**, *20*, 5969; d) M. S. Spector, J. V. Selinger, A. Singh, J. M. Rodriguez, R. R. Price, J. M. Schnur, *Langmuir*, **1998**, *14*, 3493.

[13] a) A. S. Cans, N. Wittenberg, R. Karlsson, L. Sombers, M. Karlsson, O. Orwar, A. Ewing, *Proc. Natl. Acad. Sci. USA* **2003**, *100*, 400; b) C. F. Lopez, S. O. Nielsen, P. B. Moore, M. L. Klein, *Proc. Natl. Acad. Sci. USA* **2004**, *101*, 4431; c) D. T. Mitchell, S. B. Lee, L. Trofin, N. C. Li, T. K. Nevanen, H. Soderlund, C. R. Martin, *J. Am. Chem. Soc.* **2002**, *124*, 11864.

[14] a) R. Oda, I. Huc, M. Schmutz, S. J. Candau, F. C. MacKintosh, *Nature* **1999**, *399*, 566; b) R. Oda, I. Huc, S. J. Candau, *Angew. Chem.* **1998**, *110*, 2835; *Angew. Chem. Int. Ed.* **1998**, *37*, 2689; c) D. Berthier, T. Buffeteau, J.-M. Léger, R. Oda, I. Huc, *J. Am. Chem. Soc.* **2002**, *124*, 13486.

[15] D. Vollhardt, G. Emrich, T. Gutberlet, J. H. Fuhrhop, *Langmuir* **1996**, *12*, 5659.

[16] a) T. Tachibana, H. Kambara, *J. Am. Chem. Soc.* **1965**, *87*, 3015; b) N. Nakashima, S. Asakuma, T. Kunitake, *J. Am. Chem. Soc.* **1985**, *107*, 509.

[17] W. Jin, T. Fukushima, M. Niki, A. Kosaka, N. Ishii, T. Aida, *Proc. Natl. Acad. Sci. USA* **2005**, *102*, 10801.

[18] a) Y. G. Li, T. Y. Wang, M. H. Liu, *Soft Matter*, **2007**, *3*, 1312; b) Y. G. Li, M. H. Liu, *Chem. Commun.* **2008**, 5571.

[19] a) M. M. Green, B. A. Garetz, B. Munoz, H. P. Chang, S. Hoke, R. G. Cooks, *J. Am. Chem. Soc.* **1995**, *117*, 4181; b) B. M. W. Langeveld-Voss, R. J. M. Waterval, R. A. J. Janssen, E. W. Meijer, *Macromolecules* **1999**, *32*, 227; c) J. van Gestel, *Macromolecules* **2004**, *37*, 3894; d) J. van Gestel, A. R. A. Palmans, B. Titulaer, J. Vekemans, E. W. Meijer, *J. Am. Chem. Soc.* **2005**, *127*, 5490; e) J. van Gestel, *J. Phys. Chem. B* **2006**, *110*, 4365; f) A. Lohr, F. Würthner, *Angew. Chem.* **2008**, *120*, 1252; *Angew. Chem. Int. Ed.* **2008**, *47*, 1232; g) M. M. J. Smulders, P. J. M. Stals, T. Mes, T. F. E. Paffen, A. P. H. J. Schenning, A. R. A. Palmans, E. W. Meijer, *J. Am. Chem. Soc.* **2010**, *132*, 620.

[20] a) D. L. Allara, R. G. Nuzzo, *Langmuir* **1985**, *1*, 45; b) R. G. Nuzzo, F. A. Fusco, D. L. Allara, *J. Am. Chem. Soc.* **1987**, *109*, 2358.

Received: March 7, 2010
Published online: June 2, 2010

